REVIEW
HTTP://DX.DOI.ORG/10.5504/BBEQ.2013.0106 MB
MEDICAL BIOTECHNOLOGY

APPLICATION OF FOURIER TRANSFORM INFRARED SPECTROSCOPY FOR TUMOR DIAGNOSIS

Desislava Simonova and Iliana Karamancheva
University of Chemical Technology and Metallurgy, Sofia, Bulgaria
Correspondence to: Iliana Karamancheva
E-mail: ilianak@uctm.edu

ABSTRACT

The absence of sufficient reliable methods for early detection of cancers requires a search for new and more effective techniques for screening and prevention. The discovery and introduction of appropriate techniques to test risk groups would increase the chances of successful treatment and subsequently reduce mortality. Accurate diagnostic tests and minimally invasive procedures are a main requirement for cost-effective screening tests. Fourier transform infrared spectroscopy (FTIR) is a non-invasive technology and can detect changes in a functional group in molecules from tissues or cells. The changes can be visualized by a spectrum of wavenumbers in the mid infrared range (4000 to 400 cm^{-1}). FTIR has shown promises as a sensitive diagnostic tool to distinguish malignant from normal cells in cancers including tumors of colon, ovaries, breast, skin, cervix, lung and oesophagus. The biochemical changes are often observed between tumor and normal cells within a wavenumber range known as the "fingerprint region" (encompassing 1800 to 950 cm^{-1}). The aim of this review is to summarize the application of FTIR for diagnosis of different types of cancer cells.

Biotechnol. & Biotechnol. Eq. 2013, **27**(6), 4200-4207

Keywords: FTIR spectroscopy, cancer diagnostics, early detection, absorption spectra

Abbreviations: FTIR: Fourier transform infrared spectroscopy

Introduction

Recently some spectral methods have been applied for evaluation of malignancies, and some attempts have been made to utilize some of these tests as screening techniques (4, 11, 31, 35, 36, 43). Infrared spectroscopy is a powerful tool for studies of the composition and structure of cellular components (1, 49, 50). Technological progress has enhanced the sensitivity of infrared spectroscopy, as it has further facilitated the vibrational spectra analysis, in particular the analysis of the spectral parameters such as frequency, intensity, band shape and band splitting (33, 55, 56). The main objective of this review is to evaluate Fourier transform infrared spectroscopy (FTIR) as a non-invasive, high effective and cost-advantageous method for identifying biochemical changes as biomarkers for cancer detection. The most significant differences in the spectrums of normal and cancerous tissues and cells have been observed in the wavenumber region between 400 and 4000 cm^{-1}. Thus, the mid- infrared region was reported as a major cancer diagnosis indicator (6, 7, 13, 15, 19, 21, 23, 25, 26, 34, 38, 39, 43, 46, 51, 52, 62).

Detection of a tumor in its early stage is a fundamental problem in cancer diagnosis. Surgery provides the best chance for cure if the tumor can be completely resected. Therefore, it is important to develope more accurate and sensitive diagnostic tools for early cancer detection and treatment. Histopathology is the current gold standard for cancer diagnosis, but it is highly subjective and requires the judgment of pathologists. Therefore a technique that allows a simpler, non-subjective and quicker diagnosis of cancer is needed. FTIR spectroscopy is an inexpensive technique, in support of surgeons in order to reduce the waiting time for pathological results. It can be used during or before surgical operation (27). Some of the advantages of FTIR spectroscopy are: 1) it requires only a small amount of tissue sample for analysis (29); 2) it is a reagent free technique; 3) it allows rapid and non-invasive detection of biochemical changes at the molecular level; 4) it is a computational method and evaluation can be automated which would lead to rapid and objective evaluation of the sample.

Sample preparation

One of the major advantages of FTIR spectroscopy, as a rapid and reliable method for tumor diagnosis, is the sample preparation, which is very easy and quick.

Many authors use histological smears in their research. The sample is stored in formalin and after degreasing is embedded in a paraffin block. The block is cut into thin strips with a microtome follwed by recording of spectra. However, the formaldehyde and paraffin have a strong absorption in the infrared region at 1700 cm^{-1} and 2850-2950 cm^{-1} respectively, which could lead to wrong conclusions.

Other authors simply place the sample to the ZnSe-plate without any fixative (cytological smears) and the resulting dry film is used for spectral analysis. The obtained spectrum only shows the biochemical changes in cancer tissues uninfluenced by external factors.

Human colorectal cancer analyses

Basil Rigas et. al. (42), applied FTIR to study tissue cells from human colorectal cancer. Tissue samples from colorectal cancer

and histologically normal mucosa were obtained from 11 patients who underwent partial colectomy. They used FTIR to generate absorbance spectra (frequency region 400 to 1800 cm^{-1}) to demonstrate potential metabolic differences between cells.

In the frequency region 1000-1350 cm^{-1}, they observed significant differences in the infrared spectra between normal and malignant colonic tissues. The strongest bands at 1241.0 cm^{-1} and 1082.4 cm^{-1}, due to the asymmetric and symmetric phosphate stretching modes (37) (frequencies in normal tissue), had changed intensity and shape of bands. The intensity of the $\nu_{as}PO_2^-$ band decreased, while the intensity of the $\nu_sPO_2^-$ band increased and changes in the shape of these bands in the malignant tissues were observed. In addition, the frequencies shifted to 1239.4 cm^{-1}, and 1085.1 cm^{-1} in malignant tissues. The enlarged spectra of the $\nu_{as}PO_2^-$ band, mainly originated from the phosphodiester backbone of cellular nucleic acids (32, 47, 54) for normal and malignant colonic tissues and are plotted together at **Fig. 1**.

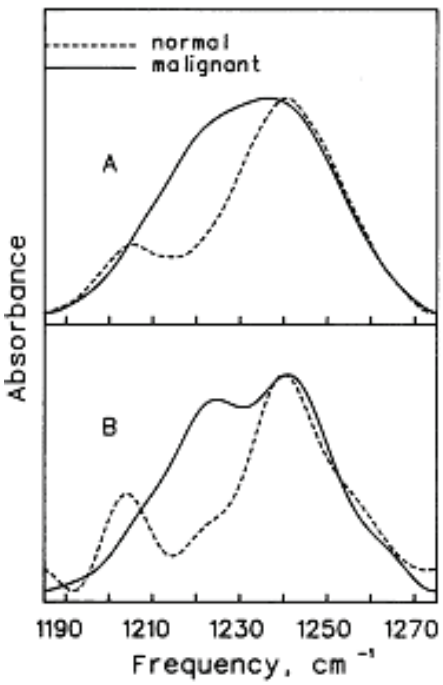

Fig. 1. Infrared spectra of a pair of normal and malignant colon tissues (frequency region: 1185-1275cm^{-1}; auto-scale plotting)

(A) Original spectra; (B) Spectra after band narrowing with Fourier self-deconvolution

Adapted from Rigas B. and Morgello S. (42)

The band at 1241 cm^{-1} in the malignant tissue after Fourier self-deconvolution splits into two at 1241.1 and 1223.8 cm^{-1}. Such splitting is barely discernible in the spectra of the normal tissue. The frequency of the asymmetric phosphate stretching mode, completely non-hydrogen-bonded, is at 1240-1260 cm^{-1} and at 1220cm^{-1} when it is fully hydrogen-bonded (10, 18). The enhance in the intensity of the band at 1223.8 cm^{-1} indicated increase in the degree of hydrogen-bonding of the oxygen atoms of the phosphate backbone of nucleic acids in the malignant colonic tissues, in contrast to normal colonic tissues (5, 57, 59). The νC-O band at 1164.2 cm^{-1} was relatively weak in the normal tissue. This band is due to the stretching mode of C-O groups in the cell proteins (5, 22, 37). In this frequency region appears the νC-O band of the acyl chains of membrane lipids, but their contribution to this band is insignificant. Therefore, the band at 1164.2 cm^{-1} in the spectra of human colon tissue is due to the νC-O mode of cell proteins (5, 59). In malignant tissues the peak maximum shifted to 1173.1cm^{-1}. The spectral changes in both, the shape and peak maximum of this band are shown at **Fig. 2**.

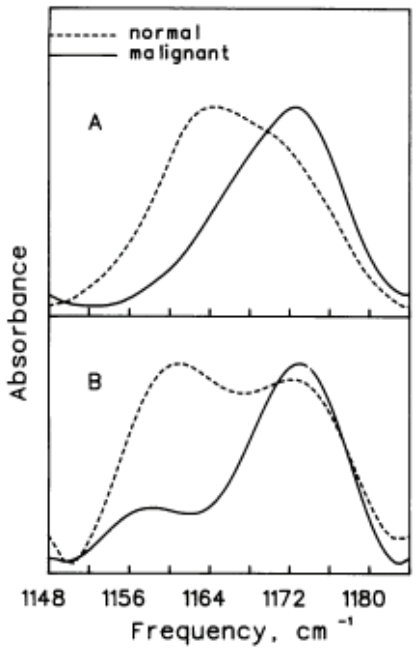

Fig. 2. Infrared spectra of a pair of normal and malignant colon tissues (frequency region: 1148-1184 cm^{-1}; auto-scale plotting)

(A) Original spectra; (B) Spectra after band narrowing with Fourier self-deconvolution

Adapted from Rigas B. and Morgello S. (42)

After self-deconvolution the spectra shows that the νC-O band consists of two overlapping bands (**Fig. 2B**). The high-frequency band is due to the νC-O mode of the non-hydrogen-bonded C-O groups in cell proteins. The band intensity of the low-frequency component is due to the νC-O mode of the hydrogen bonded C-O groups. This is dramatically decreased in malignant tissues, suggesting that in colon cancer most of the hydrogen bonds in the C-O groups disappeared.

The infrared spectra in the CH stretching mode are shown at **Fig. 3**. The bands at 2852.5 cm^{-1} and at 2958.5 cm^{-1} are due to the symmetric CH_2 stretching mode and asymmetric stretching mode, in membrane lipids. The ν_sCH_2 mode of the methylene chains and $\nu_{as}CH_3$ mode of the methyl groups shows changing in shape of the band.

The $\nu_{as}CH_3$ mode of methyl groups of membrane lipids and proteins are at about the same frequency and contribute to the intensity of the band at 2958.5 cm^{-1} (10, 37). The intensity of the $\nu_{as}CH_3$ band is decreased, and the intensity of the ν_sCH_2

band is increased in the cell spectra of human colorectal cancer and corresponding normal tissue (**Fig. 3**).

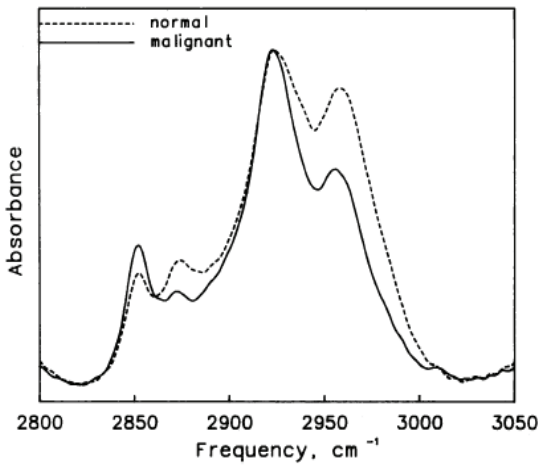

Fig. 3. Infrared spectra of a pair of normal and malignant colon tissues (frequency region: 2800-3050 cm^{-1}; auto-scale plotting)

Adapted from Rigas B. and Morgello S. (42)

Kondepati V. et al. (20) have analyzed DNA of colorectal cancer and also observed spectral differences in regions associated with nucleotide bases and the phosphodiester-deoxyribose backbone. The peaks at 1715 and 1600 cm^{-1} are due to in-plane double bond vibration of the nucleotide bases, and bands at 1500-1300 cm^{-1} represent δCH vibration and weak δNH vibration that decreases in cancer cells. The peaks at 1240 cm-1 ($\nu_{as}PO_2^-$) and 1100 cm^{-1} ($\nu_sPO_2^-$ and νCO of the deoxyribose) are strong in normal tissues but intensity decreases in the malignant samples. The peaks at 1021 and 960 cm^{-1} assigned with deoxyribose-phosphate main chain vibration are represented only as a shoulder. This suggests that structural disorders of DNA in malignant tissues are present there.

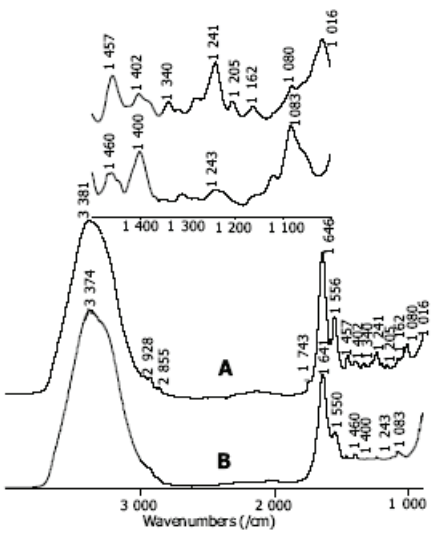

Fig. 4. Typical FTIR spectra of colon tissues measured *in vitro*

(A) Spectrum of normal colon tissue sample; (B) Spectrum of malignant colon tissue sample

Adapted from Li Q.B., Xu Z. et al. (27)

Qing Bo Li et al. (27) compared FTIR spectra of colorectal samples. They discovered that the bands due to νCH (2800-3000 cm^{-1}) and νC=O vibration (1700-1750 cm^{-1}) became weak and even disappeared in malignant tissues. As shown at **Fig. 4** the amide I band (1645 cm-1) shifted to the lower wavenumber and the intensity of the amide II band (1545cm-1) decreased and was broader in malignant tissues. The peak intensity of proteins at 1460 cm^{-1} ($\delta_{as}CH_3$) decreased, whereas at 1400 cm^{-1} (δ_sCH_3) increased.

Analyses of ovarian tumor pathology

Ovarian cancer is one of the most common gynecologic malignancy among women. Ranjana Mehrotra et. al. (41) took post surgical tissue samples from 12 patients with different grade tumors. The researchers recorded spectra of normal and malignant ovarian tissue in the mid-infrared region and observed significant differences in the frequency and intensity of proteins, nucleic acids and lipids.

The enlarged infrared spectra of the normal and malignant tissues are shown at **Fig. 5**, where the two major bands at 1078 cm^{-1} and 1238 cm^{-1}, are due to the symmetric and asymmetric stretching modes of the phosphodiester groups of cellular nucleic acids (32, 37, 47, 54).

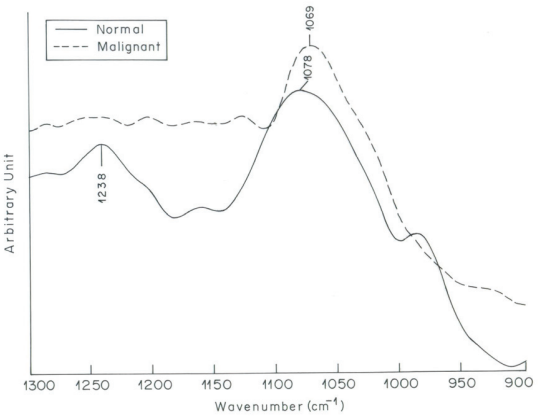

Fig. 5. Overlaid infrared spectra of normal and malignant ovarian tissue in the region 900-1300 cm^{-1}

Adapted from Ranjana M. and Gunjan T. (41)

The band at 1078 cm^{-1} of normal tissue shifted to 1069 cm^{-1} in the malignant tissue and the peak intensity increased. The asymmetric phosphate stretching vibrations at 1238cm^{-1} in normal tissue "disappeared" in the spectrum of malignant tissue (**Fig. 5**). This difference indicated the higher DNA content in malignant tissues as DNA replicates without control in cancerous cells and accumulates in larger quantities (2, 60).

In the region of amide I, II and III bands of proteins (1500-1700cm^{-1}) differences between normal and malignant ovarian tissues were also observed (**Fig. 6**).

The bands at 1630, 1642 and 1647 cm^{-1}, as well as the bands at 1536, 1543 and 1554 cm^{-1} in the amide I region of proteins are attributed to the secondary structure of proteins. The first group is due to C=O stretching vibrations of the

amide group in α-helix, whereas the absorption bands of the second group are arising from amide N-H bending vibrations in β-sheet (10, 30, 43). The vibration frequency in this region is very sensitive to changes in the molecular structure of peptide groups (10). In the malignant spectrum the bands assigned to α- and β-structures changed their intensity and peak position in comparison to normal tissue, as the increase in intensity was more prominent by β-structure. This could be attributed to conversion of α-helix to β-sheet in the malignant tissue (45, 48). Moreover, the bands in the protein region of the spectrum in normal tissues were clear whereas in the malignant ovarian tissues appeared as a broad shoulder.

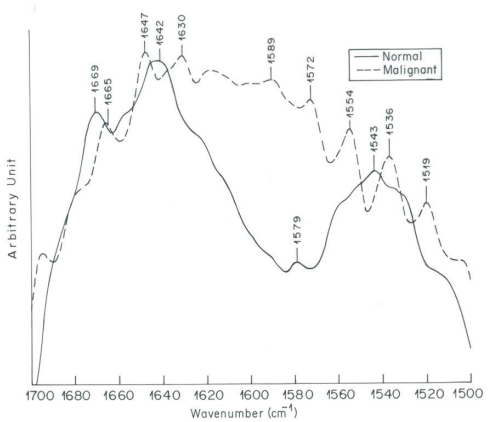

Fig. 6. Overlaid infrared spectra of normal and malignant ovarian tissue in the region1500-1700 cm^{-1}

Adapted from Ranjana M. and Gunjan T. (41)

The region 2820-2980 cm^{-1} is associated with the C-H stretching vibrations of lipids. Changes in the infrared spectra of normal and malignant ovarian tissues are also shown at **Fig. 7**. The intensity of bands at 2850 cm^{-1} and 2919 cm^{-1}, due to the CH_2 and CH_3 groups in acyl chains of lipids (10), dramatically increased in malignant tissues when compared to normal tissues.

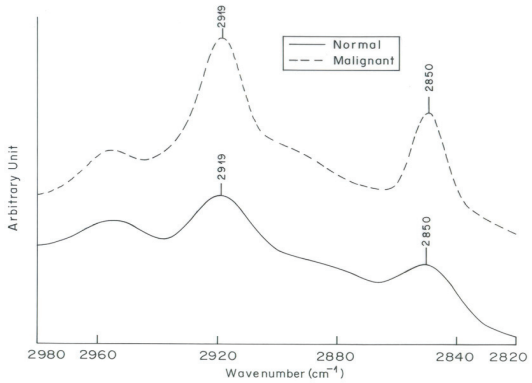

Fig. 7. Overlaid infrared spectra of normal and malignant ovarian tissue in the region 2820-2890 cm^{-1}

Adapted from Ranjana M. and Gunjan T. (41)

Analyses of cancerous tissue of the esophagus

Jian-Sheng Wang et al. (53) studied normal and cancerous tissues from the esophagus of twenty-seven patients using FTIR. The scientists determined significant differences in the FTIR spectra of proteins, sugars, fats and nucleic acids comparing normal and malignant esophageal tissues.

The protein region of the spectra showed that the amide II band at about 1550 cm^{-1} was weak and broad in malignant tissues and the intensity decreased in contrast to normal tissues. The intensity at 1645 cm^{-1} in the amide I region of proteins decreased in cancerous esophagus (**Fig. 8**).

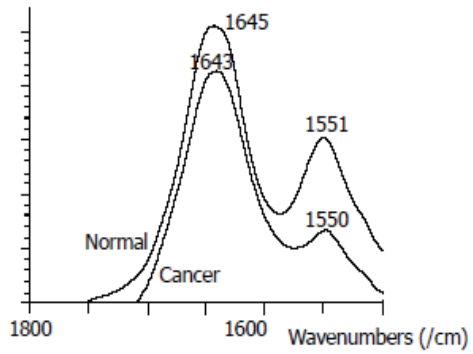

Fig. 8. The spectra of the normal and cancer tissues at 1500 - 1800cm^{-1} area

Adapted from Wang J. and Shi J. (53)

The two bands at 1453 cm^{-1} and 1402 cm^{-1} in the region 1400-1500 cm^{-1} were associated with the CH_2 and CH_3 bending vibration in acyl residues of lipids and showed changes in the infrared spectra of normal and malignant esophageal tissues. The intensity of the band at 1453cm^{-1} decreased in malignant tissues as compared to the strong and sharp band in the spectrum of normal tissues (**Fig. 9**).

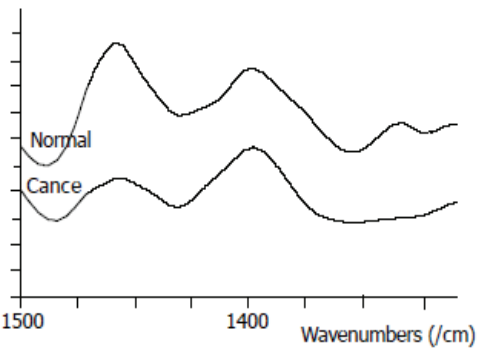

Fig. 9. The spectra of the normal and cancer tissues at 1400 - 1500cm^{-1} area

Adapted from Wang J. and Shi J. (53)

The peak at 1080 cm^{-1} due to symmetric stretching vibrations of phospholipids was higher and stronger in malignant tissues which indicated one of the most important characteristics of cancer cells: an increase in the DNA content, resulting from enhanced and uncontrolled replication of DNA.

The peak at 1745 cm^{-1} due to the νC-O band of the acyl chains of membrane lipids was observed only in 6 cases in normal tissues, but such peak was not seen in any of the samples from malignant tissues. The peaks at 2852 cm^{-1} and 2930 cm^{-1}, $\nu_s CH_2$ and $\nu_{as} CH_2$, and the peaks at 2873 cm^{-1} and

2958 cm^{-1}, $\nu_s CH_3$ and $\nu_{as} CH_3$ in membrane lipids, appeared in 25 of 27 normal tissues and in only 5 of both normal and malignant tissues.

Analyses of lung cancer

Lung cancer is one of the most common cancers worldwide. Its period of survival is poor and 90% of the patients dye within five years after they have been diagnosed. Paul Lewis et. al. (24) tried to identify the biochemical difference in sputum cells for detection of lung cancer. The researchers applied Fourier transform infrared spectroscopy as a sensitive and cost effective method. The FTIR spectra of 25 patients with lung cancer and 25 healthy controls were generated in the "fingerprint" region. The characteristic differences in the FTIR spectra from normal and cancer sputum are shown at **Fig. 10**.

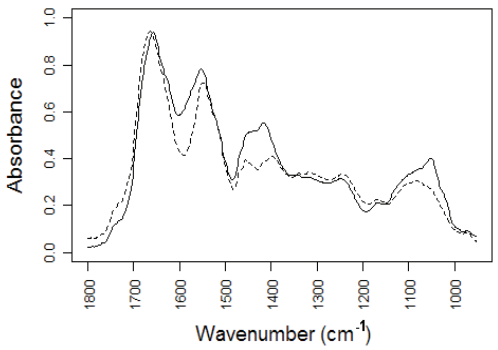

Fig. 10. FTIR spectra for normal and cancer sputum
Adapted from Lewis P. and Lewis K. (24)

The expected differences in absorbance bands between cancer and normal spectra in the region of proteins, carbohydrates and nucleic acids were confirmed (32, 47, 54). The peaks at 1656 cm^{-1} and 1577 cm^{-1} in the amide I and amide II regions in all spectra in normal and cancer cells had changed intensities. Another region of peaks with expected changes was also observed in the range from 1400 cm^{-1} to 1450 cm^{-1}, associated with bending vibration in proteins. At 1000-1100 cm^{-1} peaks of glycogen and nucleic acids were documented.

Six significant wavenumbers were summarized as a result from the analysis. The small band at 964 cm^{-1}, due to C-C stretching vibration in nucleic acids (28) and symmetrical stretching mode of dianionic phosphate monoesters of phosphorylated proteins (32) in normal samples shifted to the 966 cm^{-1} in cancer sputum.

The intensity of the peaks at 1024 cm^{-1} and 1049 cm^{-1}, associated with the C-O stretching and C-O bending vibration of glycogen (32) were increased in all cancer cells.

A previous study (63, 64) used FTIR suggested that the glycogen band in lung tumors (squamous cell carcinoma and adenocarcinoma) was increased. Wang H.P. et. al. (54) also proved that the glycogen levels were increased in lung tumor cells of pleural fluid. Consequently the increasing absorbance in glycogen rich region can be used as a biomarker for lung cancer. The COO- stretching and C-H bending vibration in proteins observed at 1417cm^{-1}, dramatically increased and shifted at 1411cm^{-1} in cancer sputum compared to a normal sample. In the region of proteins (1500-1700 cm^{-1}) an increased band absorption in the malignant cells was also observed. The band at 1656 cm^{-1} for amide I associated with νC=O vibration shifted at 1654 cm^{-1} in cancer sputum cells. The band at 1577 cm^{-1} for amide II was associated with νC-N, and δNH vibration (32). The documented infrared spectra in the protein region for adenocarcinoma and squamous cell carcinoma were the same, therefore, different types of lung cancer could not be distinguished. More detailed experiments have to be performed to detect significant wavenumbers which may be specific for lung cancer subtypes.

Analyses of breast cancer

Ranjana Mrhrotra et. al. (40) have analyzed 25 breast cancer tissues with FTIR spectroscopy. They recorded spectra of normal and malignant tissues (infiltrating ductal carcinoma, lobular carcinoma and adenomas of the breast) in the "fingerprint region" and observed the same frequency and intensity differences for proteins, nucleic acids and lipids. The representative FTIR spectra of normal control and breast cancer samples are shown at **Fig. 11**.

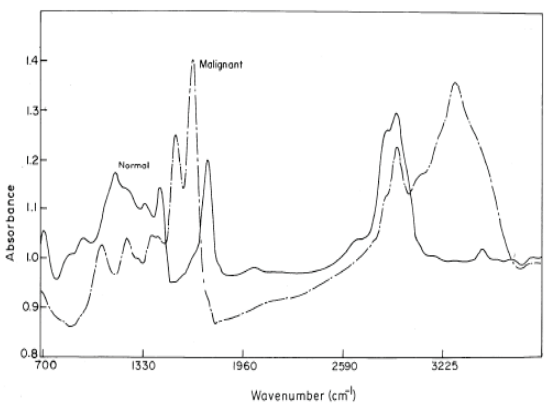

Fig. 11. Infrared spectra of normal and malignant breast tissue of a patient
Adapted from Ranjana M., Alka G et.al. (40)

The region 700-1900 cm^{-1} is mainly associated with wavenumbers for nucleic acids, phosphates, proteins and glycogen (3, 11, 14, 16). The absorbance band of $\nu_s PO^{2-}$ vibration of phosphate groups by nucleic acids shifted from 1097 cm^{-1} in the normal samples to 1076 cm^{-1} in the malignant breast tissue. The peak intensity increased in the malignant tissues relative to normal samples where it could be seen only as shoulder. The $\nu_{as} PO_2^-$ band intensity at 1258 cm^{-1} increased and shifted to 1238 cm^{-1} in breast cancer. The reason was a change in coupling of phosphate groups with alkyl groups in the malignant tissues (12). The intensity of the peak at 1157 cm^{-1}, associated with C-O bending vibration of glycogen, dramatically decreased in all cancer cells. The protein spectra (region 1300-1800 cm^{-1}) showed highly intense peaks at 1543cm^{-1} and 1653 cm^{-1} representing mainly amide II and I bands in malignant cells compared to normal tissues. The lipids band at 1359 cm^{-1} associated with δsCH_3 vibration shifted at 1396 cm^{-1} in cancer tissues and later disappeared

in the cancerous tissues. The band at 1454 cm^{-1}, for $\delta asCH_3$ vibration mode of CH_2 and CH_3 groups, and the bands at 1746 cm^{-1} ($\nu C=O$ of phospholipids esters) were also missing in the cancer spectra.

The peaks at 2849 cm^{-1} and 2932 cm^{-1} resulting from stretching vibration of CH_2 and CH_3 groups in acyl chains of the lipids or proteins showed an increased intensity in the malignant tissues. In the infrared spectra, the band at 3007 cm^{-1} was due to the symmetric CH_2 stretching and asymmetric stretching modes shifted at 3057 cm^{-1} in the breast cancer tissue suggesting changes in the membrane lipids or proteins. In the N-H region the peak at 3292 cm^{-1} was missing in the normal samples, whereas for cancer samples it was clear and strong.

Karamancheva I. et al. (17) have analyzed breast cancer with FTIR and detected characteristic bands, which could be used as biomarkers in a very rare tumor type, mucocarcinoma. For common breast tumors in the lipid regions the intensity of the bands at 2950, 2850 and 1750 cm^{-1} decreased. For the mucocarcinoma new bands at 3400 and 1300 cm^{-1} were observed resulting from formation of a muco-glycoprotein complex. This complex which contained many polysaccharide chains with only one protein had a higher molecular mass. The disorganization in the secondary structure of tumor cells was detected in the amide I region, after a curve-fit procedure. Quantitative analysis showed different ratio of α-helix, β-sheet, β-turns, random coils and that can be used for spectral diagnosis of malignancies.

Ci et al. (8) observed significant differences among normal, benign and malignant breast tumors. The analysis of fibroadenoma and carcinoma tissues revealed changes in the regions for nucleic acids and collagen proteins. The band at 970 cm^{-1} (νPO_3^{2-} - DNA and RNA ribose) was stronger and sharper for the carcinoma tissues and weaker for the benign tissue in comparison with the normal samples. Within the collagen region (1200-1400cm^{-1}) the peaks at 1204, 1280 and 1338 cm^{-1} were weaker and broader for the malignant and sharper and stronger for the benign tissues. The band of RNA ribose at 1163 cm^{-1} in the benign tissue shifted to 1171 cm^{-1} compared to the carcinoma tissue (9).

Analyses of skin cancer

Wong P et al. (58) have tested samples from basal cell carcinoma and normal skin from ten patients with FTIR spectroscopy and observed significant differences in the sample's spectra (**Fig. 12**).

The band intensity at 970 cm^{-1} that was due to symmetrical stretching mode of phosphate monoesters of phosphorylated proteins (44) and nucleic acids (60) was increased in the malignant tissues. The band at 1241 cm^{-1}, associated with $\nu_{as}PO_2$-vibration of phosphodiester groups in the nucleic acids splited into two at 1245 and 1220 cm^{-1} in the spectrum of the basal cell carcinoma. The frequency of asymmetric phosphate stretching mode, completely non-hydrogen-bonded, was at 1240 cm^{-1} and at 1220 cm^{-1} when it was fully hydrogen-bonded (48). The band at 1220 cm^{-1} indicated an increase in the degree of hydrogen-bonding of the oxygen atoms of the phosphate backbone of nucleic acids in the skin cancer samples, while in normal samples this band was missing. The intensity of the $\nu_s PO_2$ – band at 1082 cm-^{1} increased and shifted to 1086 cm^{-1} in basal cell carcinoma. The spectrum in the frequency region of 1140 to 1185 cm^{-1} (carbohydrate and cellular proteins (37) showed that the νC-O band consists of two overlapping bands, at 1163 and at 1173 cm^{-1} for the normal tissues, and 1152 and 1173 cm^{-1} for the basal cell cancer. It suggested that in skin cancer most of the hydrogen bonds in the C-O groups of cell proteins disappeared, as well as constituted some unidentified carbohydrates. The infrared spectra in the CH stretching mode showed that the band intensity at 2851 cm^{-1} due to $\nu_s CH_2$ vibration was increased and at 2958 cm^{-1} due to $\nu_{as}CH_3$ was decreased in the basal cell carcinoma.

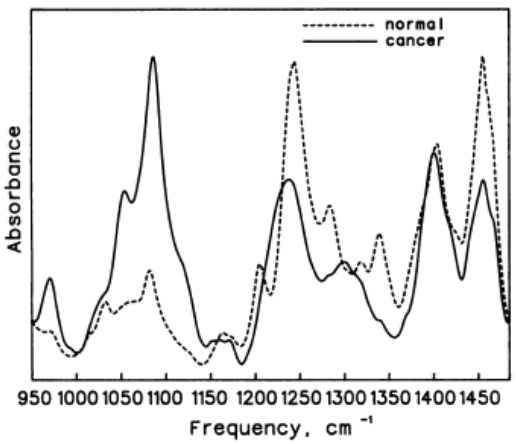

Fig. 12. Typical infrared spectra of a pair of normal skin and basal cell carcinoma from the same patient

Adapted from Wong P.T.T., Galdstein S.M. et.al. (58)

Analyses of cervical cancer

Wong P et al. (61) have analyzed samples from exfoliated cervical cells from 156 patients with FTIR spectroscopy. One hundred and thirty-six probes were determined as normal, 12 were determined to be from cervical cancer and 8 had properties of displasia. Marked differences were observed in all spectra (**Fig. 13**).

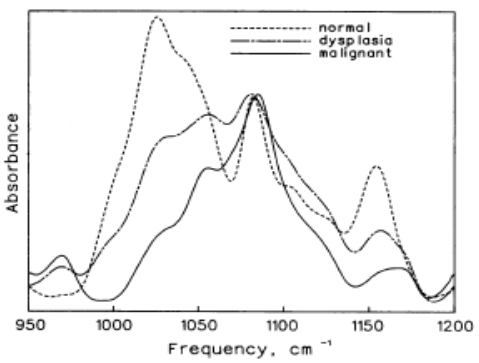

Fig.13. Infrared spectrum of a cervical sample with dysplasia
Spectra of normal and malignant cervical samples are also shown
Adapted from Wong P., Wong R. et.al. (61), with permission from AACR.

The band for $\nu_s PO_2$ – at 1082 cm^{-1} typical for normal samples, changed its intensity and shifted to 1084.4 cm^{-1} in the spectra of malignant cells. The peak intensity was also increased in the cervical samples with displasia, but the band was not shifted. The band at 1244 cm^{-1} associated with $\nu_{as} PO_2$ – vibration of phosphodiester groups in the nucleic acids was shifted and splited into two in the spectra of the cervical cancer group. The frequency of asymmetric phosphate stretching mode, completely non-hydrogen-bonded, was at 1240-1260 cm^{-1} and at 1220 cm^{-1} when it is fully hydrogen-bonded (10, 18). The enhanced band intensity indicated an increase in the degree of hydrogen-bondings that involved oxygen atoms from the nucleic acids phosphate backbone in the malignant cervical tissues, compared to the normal samples. The band at 970 cm^{-1} due to symmetrical stretching mode of phosphate monoesters of phosphorylated proteins (44) and nucleic acids (60) was missing in the normal samples, but it appeared in the malignant samples and in the samples with displasia. The band from the cervical samples with displasia was less intensive compared to that of cancer specimens. The spectra in the frequency region of 1140 to 1185cm^{-1} showed three overlapping bands with peaks centered at 1153, 1161 and 1172 cm^{-1}. The intensity of the bands at 1153 and 1161 cm^{-1}, due to stretching vibration of hydrogen-bonded C-O groups was decreased and at 1172 cm^{-1}, due to stretching vibration of non-hydrogen-bonded C-O groups was increased in the malignant cells. In addition the peak at 1153 cm^{-1} was shifted to a higher frequency region in the cancer and cervical displasia cells, but in the displasia samples the shift was less prominent. The intensity of the peaks at 1024 cm^{-1} and 1049 cm^{-1} that were associated with the C-O stretching and C-O bending vibration of glycogen (32) were decreased in both cancer and displasia cells, but the latter were characterized with a band showing an intermediate intensity.

Conclusions

The current review shows that significant difference between the infrared spectra of normal and malignant tissues and cells do exists. Depending on the type of cancerous tissue and the degree of malignancy various changes could be documented. The absorption frequencies and intensities of prominent absorption bands were changed. Differences corresponding to the content and structure of nucleic acids, lipids, proteins were observed. An increase or decrease in the levels of glycogen varied according to the cancer type. For example the levels of glycogen were higher in the lung tumor samples relative to the normal ones, but a reduction was seen in tumors of the breast. The absorption bands of proteins in some cases indicated the presence of new proteins, as well as changes in their conformation and composition. The most significant differences in the absorbance levels were observed for the symmetric and asymmetric stretching modes of phosphodiester groups of cellular nucleic acids. The observed variability differed for every particular case.

Based on the presented review we can assume that by using FTIR significant wavenumbers can be defined. These can be further used as biomarkers in tumor diagnosis. Obviously further research on different cancer cell types by means of FTIR, mainly in the characteristic "fingerprint region", but not only, can be developed as promising new tools for cancer diagnosis.

REFERENCES

1. **Auger M., Jarrell H.C., Smith I.C., Wong P.T., Siminovitch D.J., Mantsch H.H.** (1987) Biochemistry, **26**, 8513-8516.
2. **Banyay M., Sarkar M., Graslund A.** (2003) Biophys. Chem., **104**, 477-488.
3. **Bellamy L.** (1954) Infrared Spectra of Complex Molecules, John Wiley & Sons Inc., USA, p. 31.
4. **Bonnier F., Rubin S., Venteo L., Murali Krishna C., Pluot M., Baehrel B.** (2006) Biochim. Biophys. Acta, **1758**, 968-973.
5. **Cameron D.G., Moffatt D.J.** (1984) J. Testing Eval., **12**, 78-85.
6. **Chang J.I., Huang Y.B., Wu P.C., Chen C.C., Huang S.C., Tsai Y.H.** (2003) Gynecol. Oncol., **91**(3), 577-583.
7. **Chiriboga L., Yee H., Diem M., Wood B.** (2002) Gynecol. Oncol., **85**, 170-174.
8. **Ci Y., Gao T., Feng J., Gio Z.** (1999 Applied Spectrosc., **53**(3), 312-315.
9. **Demos S., Vogel A., Gandjbakhche A.** (2006) J. Mammary Gland Biol. Neoplasia, **11**, 165-181.
10. **Dukor R.K.** (2001) In: Handbook of Vibrational Spectroscopy, Volume 5 (J.M. Chalmers, P.R. Griffiths, Eds.), John Wiley & Sons Inc., New York.
11. **Franck P., Nabet P., Dousset B.** (1998) Cell Mol. Biol., **44**, 273-275.
12. **Gao T., Feng J., Ci Y.** (1999) Anal. Cell Pathol., **18**, 87-93.
13. **Gazi E., Baker M., Dwyer J., Lockyer N.P., Gardner P., Shanks J.H., Reeve R.S., Hart C.A., Clarke N.W., Brown M.D.** (2006) Eur. Urol., **50**, 750-760.
14. **Guan Y., Thomas Jr.** (1996) Biopolymers, **39**, 813-835.
15. **Haringsma J., Tytgat G.N.** (1999) Baillieres Best Pract. Res. Clin. Gastroenterol., **13**, 1-10.
16. **Jackson M., Mantsch H.** (1996) FTIR Spectroscopy in Clinical Scienses, Biomedical Application of Spectroscopy (R. Clark, R. Hester, Eds), John Wiley & Sons Inc., USA.
17. **Karamancheva I., Dobrev I., Milev A., Dimitrova M.** (2009) J. of the University of Chemical Technology and Metallurgy, **44**(3), 297-300.
18. **Kondepati V.R., Heise H.M., Oszinda T., Mueller R., Keese M., Backhaus J.** (2008) Vibrational Spectroscopy, **46**, 150-157.
19. **Kortum R.R.** (1996) Ann. Rev. Phys. Chem., **47**, 555-606.
20. **Kondepati V., Heise M., Oszinda T.** (2008) Vibrational Spectroscopy, **46**, 150-157.
21. **Krafft C., Sergo V.** (2006) Spectroscopy, **20**, 195-218.
22. **Lasch P., Haensch W., Lewis N., Kidder L.H., Naumann D.** (2002) Appl. Spectrosc., **48**, 1-10.
23. **Lasch P., Haensch W., Naumann D., Diem M.** (2004) Biochim. Biophys. Acta, **1688**(2), 176-186.

24. Lewis P., Lewis K. (2010) BMC Cancer, **10**, 640.

25. Lin S.Y., Li M.J., Cheng W.T. (2007) Spectroscopy, **21**, 1-30.

26. Li Q.B., Sun X.J., Xu Y.Z., Yang L.M., Zhang Y.F., Weng S.F., Shi J.S., Wu J.G. (2005) Clin. Chem., **51**(2), 346-350.

27. Li Q.B., Xu Z., Zhand N.W. (2005) World J. Gastroenterology, **11**(3), 327-330.

28. Malins D.C., Gilman N.K., Green V.M., Wheeler T.M., Barker E.A., Anderson K.M. (2005) Proc. Natl. Acad. Sci. USA, **102**(52), 19093-19096.

29. Malins D.C., Gunselman S.M. (1994) Proc. Natl. Acad. Sci. USA, **91**, 13038-13041.

30. Mantsch H.H., Choo-Smith L., Shaw R.A. (2002) Vib. Spectroscopy, **30**, 31-41.

31. Markovich R.J., Pidgeon C. (1991) Pharm. Res., **8**, 663-675.

32. Maziak D.E., Do M.T., Shamji F.M., Sundaresan S.R., Perkins D.G., Wong P.T. (2007) Cancer Detect. Prev., **31**, 244-253.

33. Mc Donal R.S. (1986) Anal. Chem., **58**, 1906-1925.

34. Mourant J.R., Short K.W., Carpenter S., Kunapareddy N., Coburn L., Powers T.M., Freyer J.P. (2005) J. Biomed. Opt., **10**(3), 031106.

35. Murali Krishna C., Kegelaer G., Adt I., Rubin S., Kartha V.B., Manfait M. (2006) Biopolymers, **82**, 462-470.

36. Murali Krishna C., Sockalingum G.D., Bhatra R.A., Venteo L., Kushtagi P., Pluot M. (2007) Anal. Bioanal. Chem., **387**, 1649-1656.

37. Parker F.S. (1971) Application of Infrared Spectroscopy in Biochemistry, Biology and Medicine, Plenum, New York.

38. Pikkula B.M., Shuhatovich O., Price R.L., Serachitopol D.M., Follen M., McKinnon N. et al. (2007) J. Biomed. Opt., **12**, 034014.

39. Ramanujam N. (2000) Neoplasia, **2**, 89-117.

40. Ranjana M., Alka G., Ajeet K. (2007) Indian Journal of Experimental Biology, **45**, 71-76.

41. Ranjana M., Gunjan T. (2010), Journal of Ovarian Research, **3**, 27.

42. Rigas B., Morgello S. (1990) Proc. Natl. Acad. Sci. USA, **87**, 8140-8144.

43. Sahu R.K., Mordechai S. (2005) Future Oncol., **1**(5), 635-647.

44. Sanchez-Ruiz J.M., Martinez-Carrion M.A. (1988) Biochemistry, **27**, 3338-3342.

45. Sheeler P., Bianchi D.E. (1980) Cell Biology, John Wiley and Sons Ink., New York.

46. Sokolov K., Follen M., Kortum R.R. (2002) Curr. Opin. Chem. Biol. **6**, 651-658.

47. Stuart B.H. (2004) Infrared Spectroscopy: Fundamentals and Applications, John Wiley & Sons Inc., New York.

48. Swai H., Timasheff S.N. (1969) In: Structure and Stability of Biological Macromolecules (G.D. Fasman, Ed.), Dekker, New York, 641-659.

49. Takahashi H., French S.W., Wong P.T.T. (1989) Hepatology, **10**, 705.

50. Takahashi H., French S.W., Wong P.T.T. (1991) Alcohol Clin. Exp. Res., **15**, 219-223.

51. Tfayli A., Piot O., Durlach A., Bernard P., Manfait M. (2005) Biochim. Biophys. Acta, **1724**, 262-269.

52. Wagnieres G.A., Star W.M., Wilson B.C. (1998) Photochem. Photobiol., **68**, 603-632.

53. Wang J., Shi J. (2003) World Journal of Gastroenterology, **9**(9), 1897-1899.

54. Wang H.P., Wang H.C., Huang Y.J. (1997) Sci. Total. Environ., **204**, 283-287.

55. Wong P. (1987) Current Perspective in High Pressure Biology (R.E. Margulis, Ed.), Academic Press, London, 287-314.

56. Wong P. (1987) High Pressure Chemistry and Biochemistry (R. Eldik, J. Jonas, Eds.), Reidel, Dordrecht, The Netherlands, NATO ASI Ser. C, **197**, 381-400.

57. Wong P.T.T. (1987) Vibrational Spectra and Structure (J.R. Durig, Ed.), Elsevier, Amsterdam, **16**, 357-445.

58. Wong P.T.T., Goldstein S.M., Grekin R.C., Godwin T.A., Pivik C., Rigas B. (1993) Cancer Research, **53**, 762-765.

59. Wong P.T.T., Mantsch H.H. (1988) Chem. Phys. Lipids, **46**, 213-224.

60. Wong P.T.T., Papavassiliou E.D., Rigas B. (1991) Appl. Spectrosc., **45**(9), 1563-1567.

61. Wong P., Wong R., Caputo T. (1991) Proc. Natl. Aca. Sci. USA, **88**, 10988-10992.

62. Yang Y., Sule-Suso J., Sockalingum G.D., Kegelaer G., Manfait M., El Haj A.J. (2005) Biopolymers, **78**(6), 311-317.

63. Yano K., Ohoshima S., Gotou Y., Kumaido K., Moriguchi T., Katayama H. (2000) Anal. Biochem., **15**, 218-225.

64. Yano K., Ohoshima S., Shimizu Y., Moriguchi T., Katayama H. (1996) Cancer Lett., **110**, 29-34.